

An algorithm-based method for accurate compensation of bandgap references over temperature

Madalina BONCU^{1,2}, Catalin BOTEZATU¹, and Florin DRAGHICI²

¹ON Semiconductor Romania

²Politehnica university of Bucharest, Romania

E-mail: boncumadalina@yahoo.ro, catalin.botezatu@onsemi.com,
florin.draghici@upb.ro

Abstract. A curvature-compensated bandgap voltage reference circuit, with a high degree of temperature compensation, is designed and implemented in a $0.18\mu\text{m}$ CMOS technology.

The accuracy of the circuit was obtained with the help of a software code, having the aim of calculating the necessary parameters. Thus, a newly design method, implemented in MATLAB[®] software, is proposed.

The circuit is intended for integration within a voltage regulator with an adjustable output voltage. The bandgap circuit provides a reference voltage of 1.2V, for supply voltages between 1.65V and 3.6V, over a temperature range of -40°C to 85°C . The targeted TC is below $10\text{ ppm}/^{\circ}\text{C}$ for typical process parameters.

Key-words: Bandgap Voltage Reference (BVR), Curvature compensation, Temperature coefficient (TC), Proportional To Absolute Temperature (PTAT), Complementary To Absolute Temperature (CTAT).

1. Introduction

This paper is an extended version of [1] and presents an accurate method for compensating bandgap references over temperature.

A BVR is an electronic circuit that is crucial in many analog, mixed-signal and memory applications, the demand for biasing circuit being present in almost every integrated device. It produces a constant reference voltage regardless of power supply voltage, temperature, and process variations. It commonly has an output voltage around the theoretical 1.2 V diode voltage at 0 K [2, 3].

The proposed bandgap reference is intended to be integrated inside a voltage regulator with a digital controlled output voltage. The bandgap voltage is used as a reference for this circuit.

One of the most important parameters of this electronic circuit is TC, since it directly affects the accuracy of the system in which it is included. The TC defines the change in the reference voltage given by the temperature variation, and it is usually measured in ppm/°C. The necessity of a low TC involves the development of new temperature-compensation techniques.

The implementation of the temperature compensation techniques increases the complexity of the schematic. Supplementary circuits are introduced, thereby leading to numerous parameters that have to be carefully chosen for achieving the desired functionality. Therefore, the automation of the design process would be an important starting point for the design of the circuit.

The presented method is enhanced by an algorithm coded in MATLAB software, in order to achieve optimal results.

2. Principle of operation

The bandgap voltage reference architecture is illustrated as a block diagram in Fig. 1. Thus, the whole circuit is divided into six sub-circuits (start-up, bias, core, OTA - operational transconductance amplifier, curvature compensation and the output stage). Each of these sub-circuits performs a well-determined function which allows the BVR to work correctly.

The start-up circuit has the role of providing an impulse to the reference circuit, in order to reach the desired equilibrium state, at which the reference voltage has the expected value of 1.2V.

The biasing block provides a current to power on the BVR, and this will be further implemented through a Widlar current source.

The BVR core is created by summing two terms with complementary temperature coefficients. The PTAT voltage is generated by measuring and scaling the difference between two forward-biased emitter-base voltages, while the CTAT term is generated using an emitter-base voltage under forward bias condition [4].

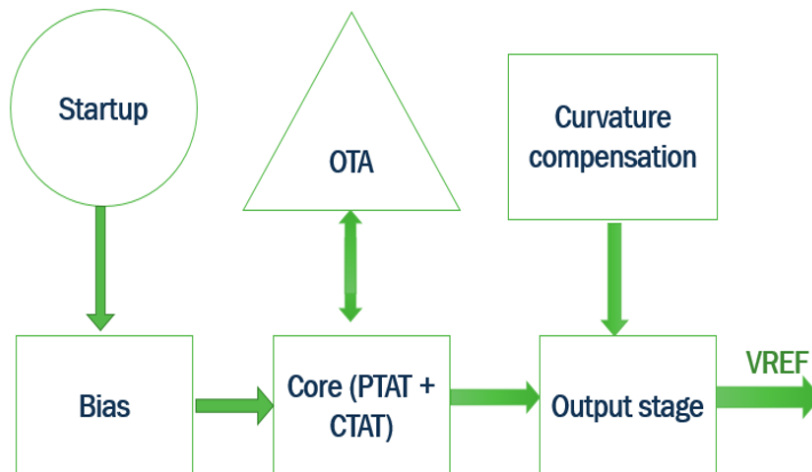


Fig. 1. The block diagram of the reference circuit.

A circuit implemented this way offers a reference voltage by adding the PTAT and CTAT terms, ideally leading to a zero temperature coefficient.

However, the base-emitter voltage does not have a linear dependence with temperature, its expression inherently containing a logarithmic temperature-dependent term, as shown in (1).

$$V_{BE} = V_{G0} - \frac{V_{G0} - V_{BE}(T_0)}{T_0} \cdot T - (a - b) \cdot V_{th} \cdot \ln\left(\frac{T}{T_0}\right) \quad (1)$$

where V_{G0} is the bandgap voltage of Silicon extrapolated at 0K, T is the absolute temperature in degrees Kelvin (K), V_{th} is the thermal voltage, T_0 is the reference temperature, a and b are temperature dependent parameters of silicon mobility and the collector current that provides V_{BE} from (1).

The core (Fig. 1) only compensates the linear term from this formula, by adding a component that increases linearly with temperature.

Nevertheless, the temperature coefficient would have a high value because the nonlinear term was not compensated. This paper aims to modify the conventional 1st order compensated waveform and to obtain a higher order one, thereby achieving a lower temperature coefficient. Consequently, the use of a nonlinear temperature dependent term is absolutely necessary. The curvature correction block, shown in the above diagram, has the role of lowering the TC value. In this work, the used compensation method is based on the piecewise-linear technique [2]. It uses the nodal subtraction of currents, as shown in Fig. 2.

For the lower half of the temperature range, PTAT current ($k_1 \cdot I_{PTAT}$) is less than CTAT ($k_2 \cdot I_{CTAT}$) current, Q_1 PMOS transistor operates in the linear region and Q_2 is turned off (nonlinear current is zero) [2].

For the upper half of the temperature range, PTAT current becomes larger than the CTAT current, Q_1 is saturated, thereby forcing Q_2 to source the difference between the currents [2].

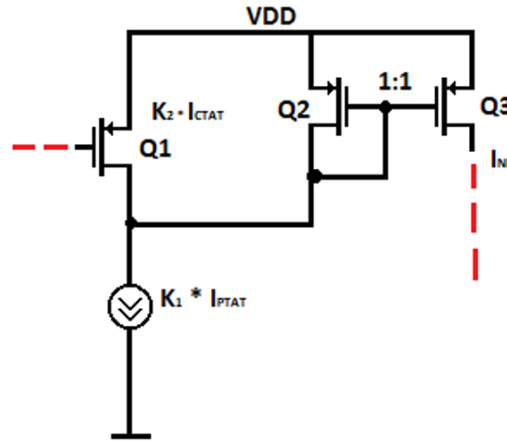


Fig. 2. Piecewise-linear curvature-correcting current generator.

The nonlinear current (I_{NL} , sourced by Q_3) formula is described by (2) [2].

$$I_{NL} = \begin{cases} 0, & I_{ctat} \geq I_{ptat} \\ k_1 I_{ptat} - k_2 I_{ctat} & I_{ctat} < I_{ptat} \end{cases} \quad (2)$$

Moreover, the intersection point between PTAT and CTAT currents also represents the point where the nonlinear current starts to become non-zero, this being the starting point for the curvature correction.

To define this point, two additional coefficients (k_1 and k_2) appear for each nonlinear current. Those coefficients are set through the aspect ratio of current mirrors.

The output stage consists of a current-voltage converter, composed of three resistors, as it can be observed in Fig. 3.

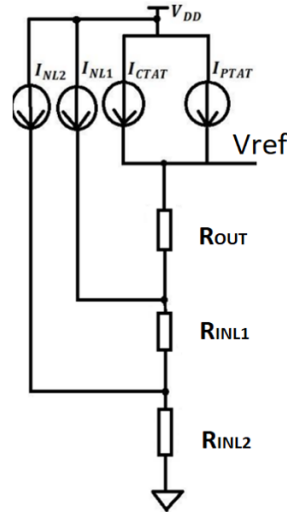


Fig. 3. BVR output stage.

It provides a reference voltage given by the following expressions:

$$V_{REF} = (I_{ptat} + I_{ctat}) \cdot R_{OUT} + (I_{ptat} + I_{ctat} + I_{INL1}) \cdot R_{INL1} + (I_{ptat} + I_{ctat} + I_{INL1} + I_{INL2}) \cdot R_{INL2} \quad (3)$$

The complete circuit of the BVR is depicted in Fig. 4.

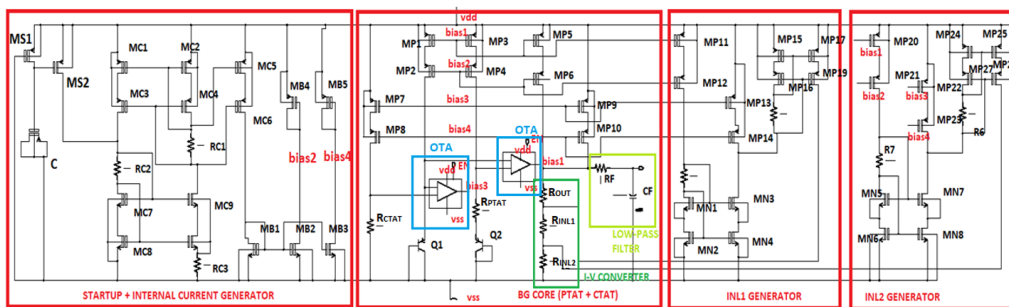


Fig. 4. The proposed schematic of BVR.

The PTAT current is provided through the difference of Q1 and Q2 emitter-base voltages, referred to R_{PTAT} , whereas the CTAT voltage is given by the base-emitter voltage of Q1 transistor,

divided by R_{CTAT} .

By replacing the two currents, equation (3) becomes:

$$V_{REF} = \left(\frac{V_{eb1} - V_{eb2}}{R_{PTAT}} + \frac{V_{eb1}}{R_{CTAT}} \right) \cdot R_{OUT} + \left(\frac{V_{eb1} - V_{eb2}}{R_{PTAT}} + \frac{V_{eb1}}{R_{CTAT}} + I_{NLI} \right) \cdot R_{INLI} + \left(\frac{V_{eb1} - V_{eb2}}{R_{PTAT}} + \frac{V_{eb1}}{R_{CTAT}} + I_{NLI} + I_{NLI2} \right) \cdot R_{INLI2} \quad (4)$$

It can be observed in Fig. 4 that two blocks were used for generating the nonlinear currents. The purpose is to reduce TC by dividing the temperature range into three consecutive segments, as it is illustrated in Fig. 5. The reference voltage variation can be further reduced when more segments are considered, but the disadvantages are increased area and current consumption.

In order to split the V_{ref} 1st order curve into N adjacent curves (which will have reduced variation), it is necessary to introduce N-1 nonlinear currents.

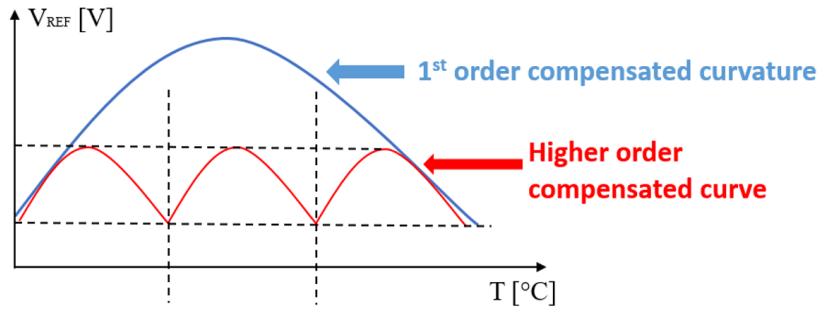


Fig. 5. Illustration of the proposed technique principle.

A total number of nine coefficients were introduced, four parameters being used for the generation of the two nonlinear currents ($k_1 - k_4$), and also five coefficients for the values of the resistors (R_{PTAT} , R_{CTAT} , R_{INLI} , R_{INLI2} and R_{OUT}). As it can be observed in equation (4), the 5 resistors are highly correlated. The PTAT and CTAT resistors are directly proportional, the higher the PTAT resistance, the higher the R_{CTAT} must be, so that the currents intersect in the middle of the temperature range. R_{OUT} is directly proportional to R_{PTAT} and R_{CTAT} . To obtain the same reference voltage, an increase or decrease of the R_{PTAT} and R_{CTAT} resistors leads to an increase or decrease of the R_{OUT} resistance. The 2 nonlinear resistors are directly proportional to all resistors discussed above, as can be seen in (4). k_1 and k_2 coefficients are inversely proportional, as can be seen in equation (2). To obtain a given nonlinear current, an increase in k_1 coefficient leads to an increase in k_2 coefficient. k_3 and k_4 coefficients are independent of k_1 and k_2 but dependent on each other. All those parameters have to be carefully chosen for achieving an optimal design.

3. MATLAB calculation results

As it was described above, the purpose is to automate the design process, by creating the MATLAB software code to calculate the desired coefficients.

In this code, the reference voltage computed by the created program code was also plotted and compared to the targeted waveform presented in section 2 (Fig. 5).

For achieving the targeted results, the theoretical formulas and techniques were analysed, which make possible the obtainment of the superior order curve.

As it was presented in Fig 5, the waveform of the reference voltage will be considered as being composed of three subintervals, on each sub-range the waveform being similar to the 1st order waveform.

The algorithm starts with the implementation of PTAT and CTAT formulas and the declaration of the required variables. Fig. 6 illustrates the workflow diagram of this code.

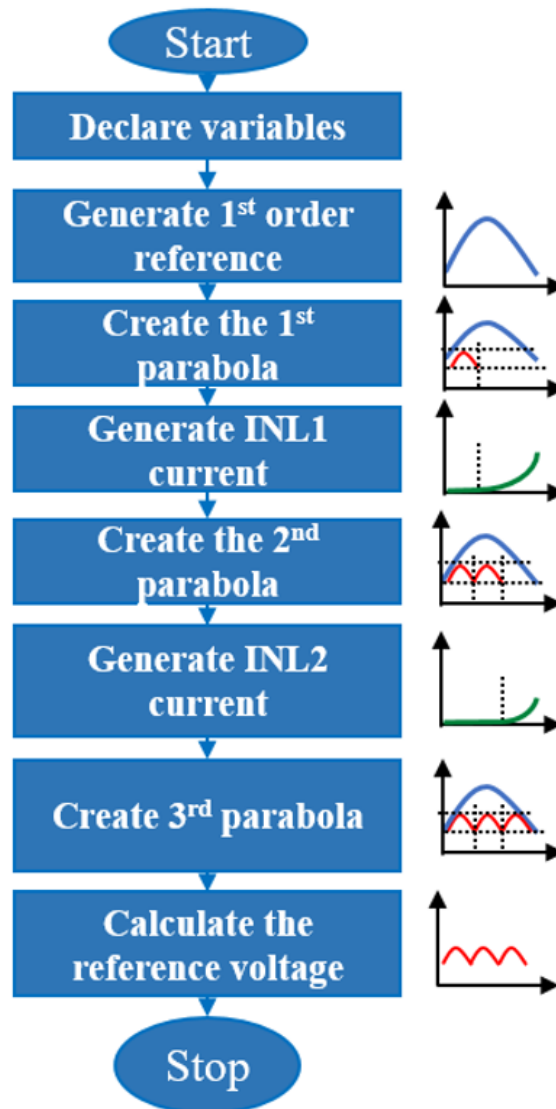


Fig. 6. The workflow diagram of the code.

The first step in the coding process was the implementation of base-emitter formula and the theoretical calculation of CTAT and PTAT voltages. The formula has been implemented in order to make the CTAT voltage slope to be around the theoretical value of $-2\text{mV}/^\circ\text{C}$ under temperature analysis.

After defining these voltages, the computation of the 1st order characteristic has begun, being the starting point of this algorithm.

When dealing with a 1st order curvature compensation, it is important that the slopes for both CTAT and PTAT voltages are complementary within a certain accuracy, as shown in Fig. 7. In this figure, several lines with different slopes can be observed. Initially, the slopes for CTAT and PTAT are not complementary and are shown in Fig. 7 with light green and blue colors. Therefore, in order to obtain a reference voltage with reduced TC, at least the PTAT line should be multiplied with a coefficient ($a1$ in this case).

In reality, the reference voltage will not be a straight line, its shape being rather a parabola. The reason why the slopes have to be complementary is that the parabola which is corresponding to the 1st order curve must have the maximum value at the central point of the temperature range. Moreover, the values at the beginning and end points of the temperature range should be equal. This leads to a symmetrical waveform, with a reduced temperature coefficient. If the slopes are not equal, the waveform tends to follow a CTAT or PTAT shape. For this purpose, the value of a resistor was adjusted using a “while” type loop. The accuracy mentioned above is set by the step by which the resistor is varied inside this code, in this case having the value of 1Ω , as it will be observed from the logic diagram. If this step for the resistor is too large, the 1st order curve will not be obtained.

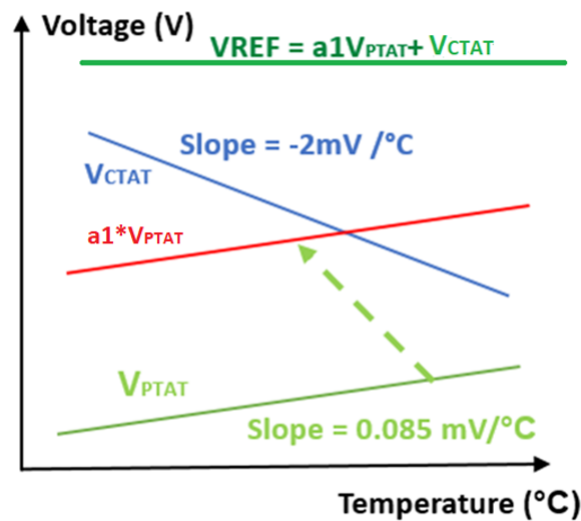


Fig. 7. The slopes for PTAT and CTAT.

At the beginning, a higher value for this RPTAT resistor was preferred, to make sure that PTAT slope value is always smaller than CTAT slope. Then, the slopes for PTAT and CTAT components are calculated. While those 2 values are different from each other and if the negative value of the CTAT slope is larger than the PTAT one, PTAT resistance is decremented. PTAT slope is calculated again until the condition is met.

R_{OUT} resistance was chosen in order to obtain a value of 1.2V for the reference voltage at the nominal temperature of 25°C. As it was presented in [2], this value is the diode voltage at 0K.

The logic diagram corresponding to this step and the computation result can be seen in Fig. 8, being the second step of the algorithm.

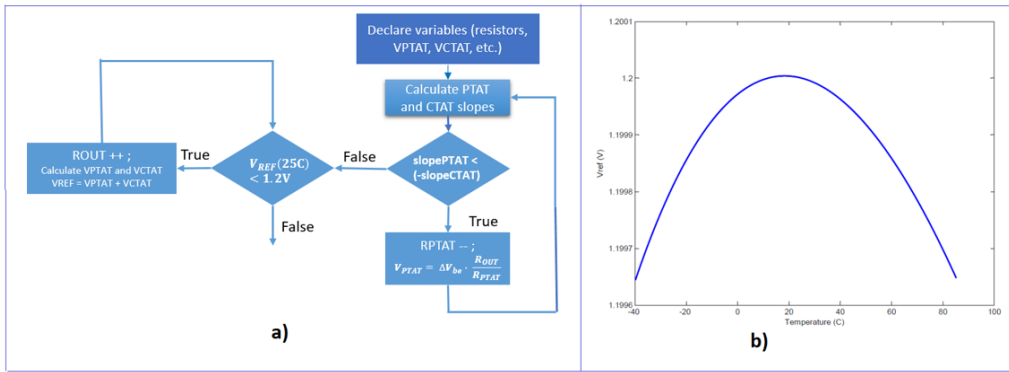


Fig. 8. First order voltage characteristic. a) Logic diagram, b) Computation result.

As can be observed from Fig. 8b, the first order reference curve has been obtained.

For the third step, the first parabola of the reference voltage is created as it can be depicted in Fig. 9. The beginning and the end points of the section are given by the corresponding temperature for the first index of the temperature vector and the temperature corresponding to the length of the vector divided by three, respectively. The first parabola is created when the reference voltage values from the beginning and the end points of the subinterval are equal.

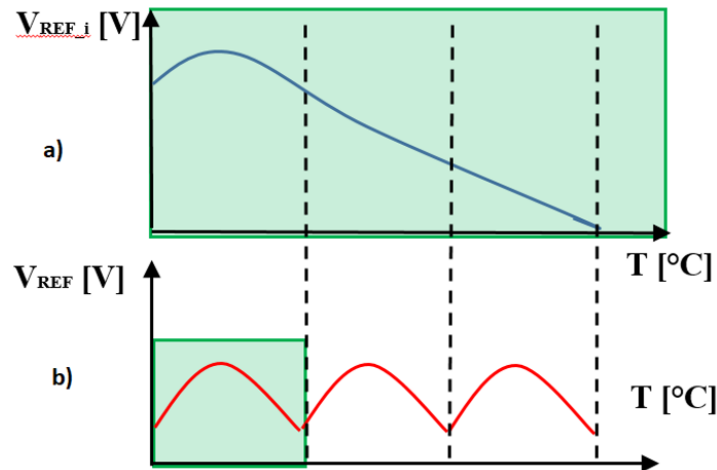


Fig. 9. Creation of the 1st parabola of the reference voltage. a) The first parabola, b) The targeted reference voltage.

In order to achieve the superior order curve, the calibration for R_{PTAT} was chosen, until the extremes of the interval are equal.

Fig. 10a shows the logic diagram of this algorithm, which was coded in MATLAB software. Also, the result shown in Fig. 10b has the expected waveform.

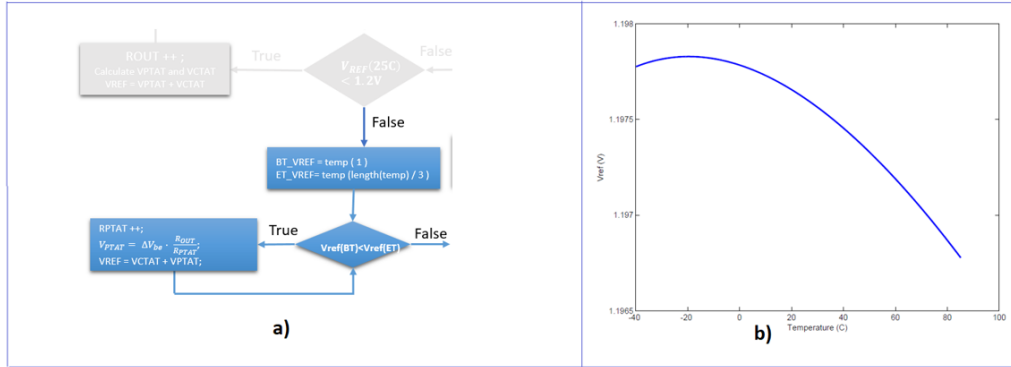


Fig. 10. First parabola in the final reference voltage. a) Logic diagram b) Computation result.

For the generation of nonlinear currents, piece-wise linear technique, presented in reference [2], was used. Nonlinear currents start to become non-zero at the point where PTAT and CTAT currents are equal. k_1 and k_2 coefficients are initially set to a value of one and then one of the parameters is modified until the aforementioned point is reached.

Fig. 11a illustrates the logic diagram of this part, along with the waveform obtained in MATLAB program (Fig. 11b).

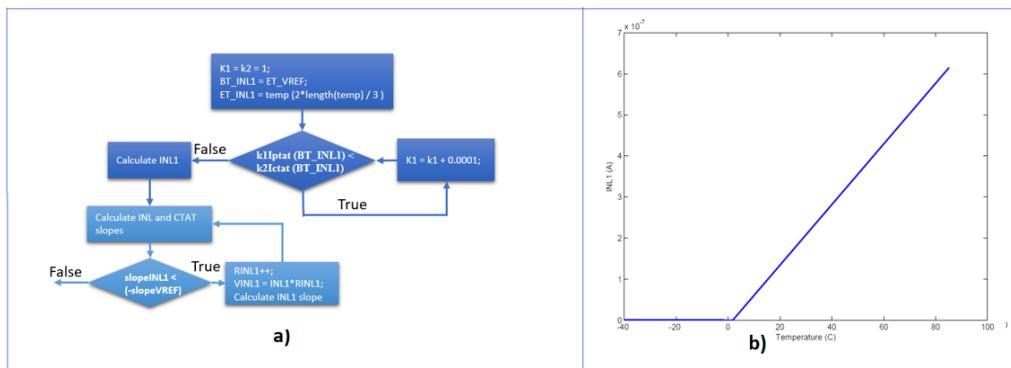


Fig. 11. The generation of the 1st nonlinear current. a) Logic diagram b) Computation result.

For the second nonlinear current, the generating method is similar to the one for the 1st current, but the main difference is that the initial PTAT current is higher than CTAT current and k_3 coefficient should be decremented instead of incremented (Fig. 12a). The waveform illustrated in Fig. 12b has the expected shape.

As it can be seen from Figs. 11b and 12b, the nonlinear currents were correspondingly generated, those having the role of setting the points in which the curve will be compensated using the nonlinear components.

The last step is the calculation of the reference voltage, shown in this Fig. 13. It can be observed that this waveform generated by the program is similar to the targeted one.

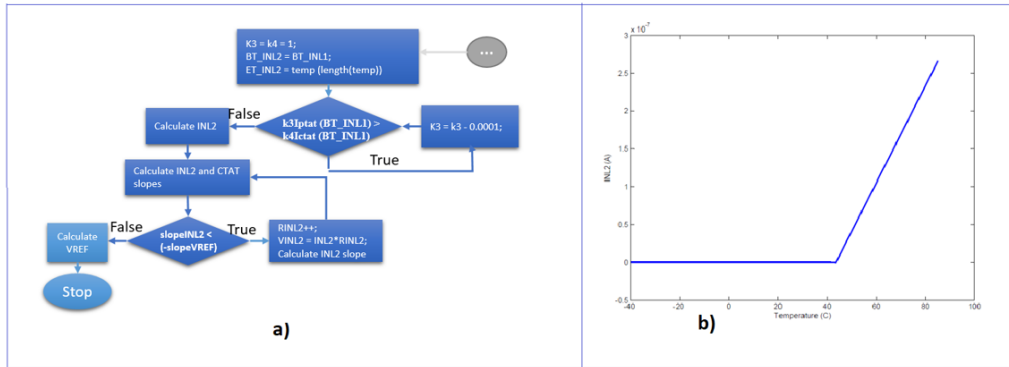


Fig. 12. The generation of the 2nd nonlinear current a) Logic diagram b) Computation result.

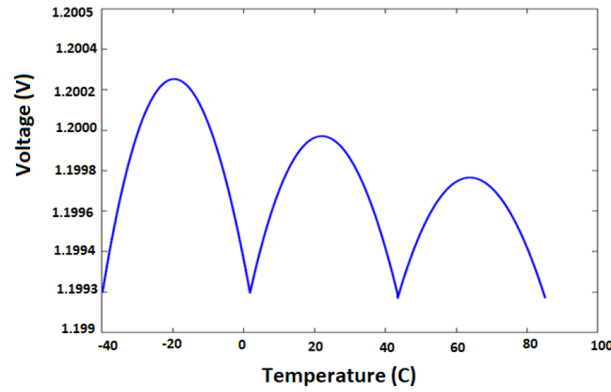


Fig. 13. The final reference voltage.

Thus, the desired waveform was obtained. It is a higher order waveform, presenting all three sub-intervals.

Even though this algorithm does not take into consideration all the side effects that can appear, this is a good starting point for design. Therefore, a few design adjustments could be considered in order to obtain the desired results.

The two main advantages of this code are: it reduces the simulation time and gives the best results.

4. Circuit implementation and simulation results

In the table below the design requirements as well as simulations conditions are illustrated. It is desired to obtain a reference voltage of 1.2V, for supply values starting from 1.65V up to 3.6V and over a temperature range from -40°C to 85°C . Also, the desired TC is less than $20\text{ppm}/^{\circ}\text{C}$, the total current consumption of maximum $25\ \mu\text{A}$ and the line sensitivity of $0.5\%/V$.

Table 1. Design requirements and simulations conditions

Parameter	Design specifications
Vref	1.2V
Temperature range	-40°C ÷ 85°C
Supplyrange (VDD)	1.65V ÷ 3.6V
TC	< 20ppm/°C
Totalcurrent consumption (Icc)	< 25μA
Line sensitivity (LS)	0.5%/V

4.1. Temperature analysis

The circuit was designed and implemented in an 180nm CMOS technology and the simulations were realized using Pyxis™ program package.

The different operating temperatures in which the system works might impact the performance of every component in the circuit, making the reference voltage (VREF) a temperature-dependent signal. [5] The metrics of this behaviour is referred as temperature coefficient (TC) and it is given by (5):

$$TC = \frac{(V_{REFmax} - V_{REFmin})}{(T_{max} - T_{min}) \cdot V_{REF,25C}} = \frac{\Delta V_{REF}}{\Delta T \cdot V_{REF,25C}} \cdot 10^6 \quad (5)$$

where ΔT represents the variation of temperature and $\frac{\Delta V_{REF}}{V_{REF,25C}}$ is the reference voltage variation referred to its nominal value, measured at 25°C. The typical measuring unit for this parameter is parts-per-million per degree Celsius (ppm/°C).

Temperature analysis was realized by varying the temperature from -40°C up to 85°C. Fig. 14 shows the reference voltage waveform for a supply voltage of 1.8V. For this particular case, a temperature coefficient of 5.9 ppm/°C was obtained.

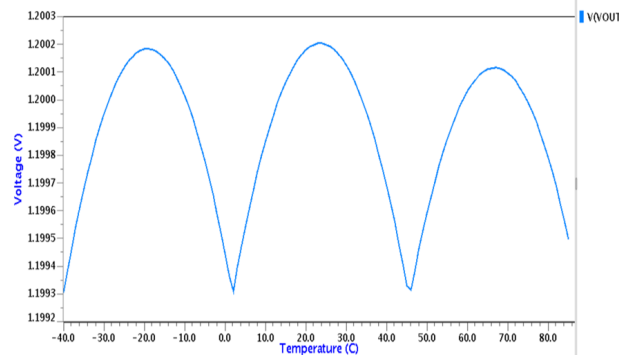
**Fig. 14.** The reference voltage for a supply value of 1.8V.

Fig. 15 shows a more detailed analysis of BVR working principle. In Fig. 15a the reference voltage in the absence of nonlinear currents is presented. Furthermore, the I_{NL1} and I_{NL2} currents are shown in Fig. 15b and Fig. 15c, respectively. As it can be observed in Fig. 15d,

the reference voltage obtained by weighted summing of the components presented above, has a small voltage variation over the entire temperature range.

For the 1st temperature range, between -40°C and 2°C , the reference behaves similarly to a first order compensated reference, due to the fact that the nonlinear currents are 0A. For the 2nd temperature range, between 2°C and 46°C , the voltage reference is mainly compensated due to the presence of INL1 current. Moreover, for the 3rd temperature range, higher than 46°C , the compensation of the reference voltage is obtained based on I_{NL1} and I_{NL2} currents.

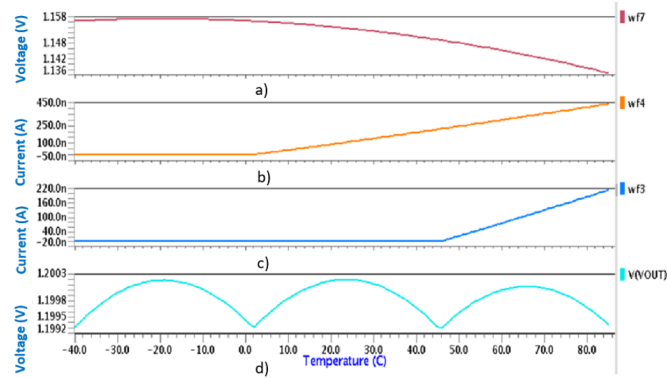


Fig. 15. The complete illustration of the proposed technique. a) Vref in absence of nonlinear currents b) INL1 current c) INL2 current d) Compensated Vref .

In Fig. 16 the dependence of the reference voltage on the supply voltage is presented. The reference voltage has a minimal dependence on the supply voltage, being capable of keeping a reduced TC.

For supply voltages starting from 1.75V, all the curves are showing the same reduced variation with temperature for the reference voltage, while for the supply voltage of 1.65V the reference voltage has a larger variation because the BVR is at its working limit.

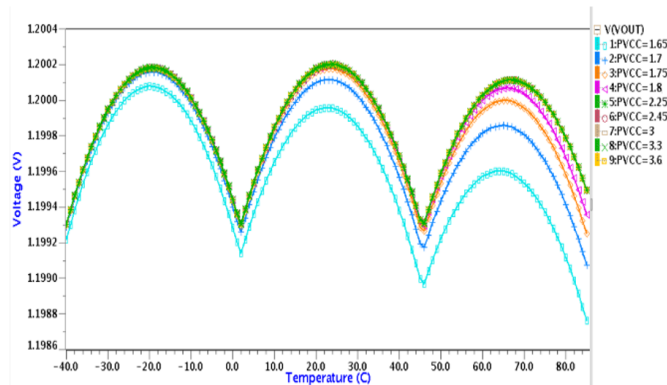


Fig. 16. The reference voltage for multiple supply values.

In Table 2, the TC for multiple supply values is shown. A maximum TC of $8.76\text{ppm}/^{\circ}\text{C}$ is obtained for a supply voltage of 1.65V, being under the targeted value.

Table 2. TC for multiple supply values

VDD [V]	V _{REF(max)} [V]	V _{REF(min)} [V]	V _{REF(25°C)} [V]	TC [ppm/°C]
1.65	1.2001	1.1988	1.1999	8.7681
1.7	1.2002	1.1991	1.2001	7.2252
1.75	1.2002	1.1993	1.2002	6.1697
1.8	1.2002	1.1993	1.2002	5.9832
2.25	1.2002	1.1993	1.2002	5.9803
2.45	1.2002	1.1993	1.2002	5.9825
3	1.2002	1.1993	1.2002	5.9869
3.6	1.2002	1.1993	1.2002	5.9874

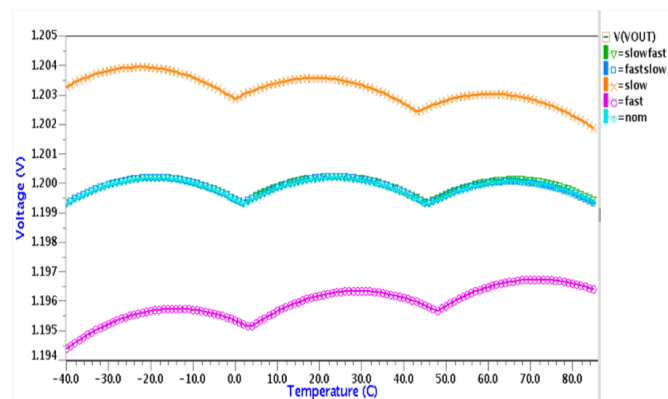
Another simulation of major importance is implemented by considering multiple process corners (Fig. 17).

In Table 3 all the TC values for all the process corners can be observed, for a supply voltage of 1.8V.

Table 3. TC over process corners

Process corner	V _{REF(max)} [V]	V _{REF(min)} [V]	V _{REF(25°C)} [V]	TC [ppm/C]
slowfast	1.2002	1.1993	1.2002	6.046
fastslow	1.2002	1.1993	1.2002	6.034
slow	1.2039	1.2019	1.2035	13.709
fast	1.1967	1.1944	1.1963	15.735
nom	1.2002	1.1993	1.2002	5.9832

For nominal, slowfast and fastslow corners, the reference voltage curves, shown in Fig. 17, are perfectly overlapping (V_{ref} variation is reduced), while for slow and fast corners there is a deviation from the typical curve, but still keeping the nonlinear characteristic of the curve.

**Fig. 17.** V_{ref} for multiple process corners, v_{dd}=1.8V.

Another important parameter for the BVR is the total current consumption. The quiescent current increases with the rise of the temperature due to the appearance of nonlinear currents.

Fig. 18 shows the total current consumption of the circuit for all process corners and a supply voltage of 3V. This parameter has a minimum value of $17\mu\text{A}$ whereas the current reaches a maximum of $22\mu\text{A}$.

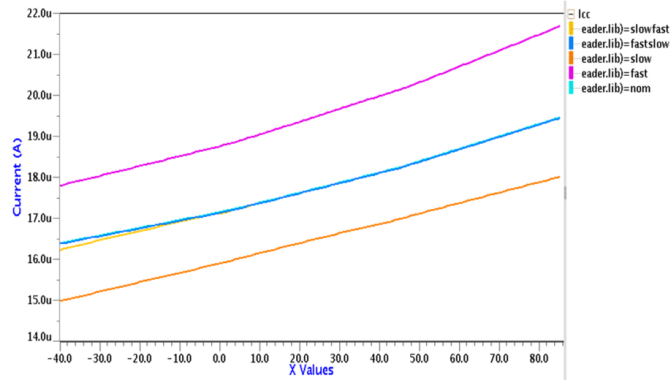


Fig. 18. The quiescent current for the BVR.

4.2. DC analysis

Line sensitivity (LS) measures the relative variation of the reference voltage when the supply voltage is changed.

This analysis was made by varying the supply voltage from 0V to 5V and observing the reference voltage. Line sensitivity was calculated within the specified input voltage range (from 1.65V up to 3.6V).

In Fig. 19 it can be observed the reference voltage versus the supply voltage, for all PVT (Process-Voltage-Temperature) conditions. The circuit starts working correctly from a voltage close to 1.65V, this being the working limit for the BVR.

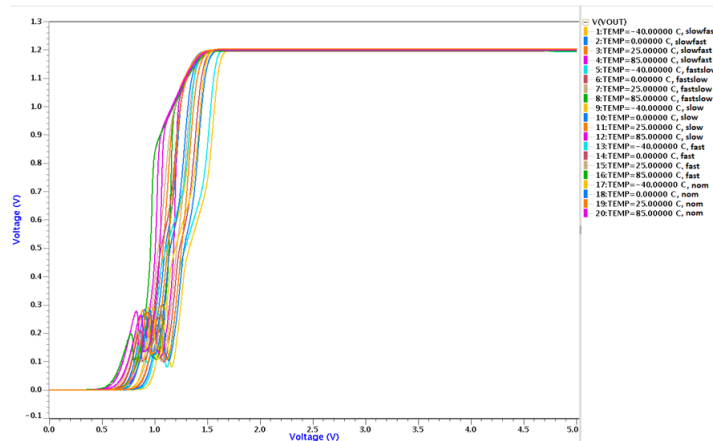


Fig. 19. The reference voltage vs supply voltage.

The results for line sensitivity were listed in the table below, for all PVT conditions. For the nominal corner, a value of 41.11 ppm/V was achieved for this parameter, whereas the worst-case value is 85.4 ppm/V, the circuit having a reduced variation when modifying the supply voltage.

Table 4. Line sensitivity results

Corners	Temp [C]	LS [ppm/V]	VREF_3p6V [V]	VREF_1p8V [V]
slowfast	-40	-1.3219	1.1993	1.1993
slowfast	0	-1.0676	1.1994	1.1994
slowfast	25	1.2339	1.2002	1.2002
slowfast	85	34.6511	1.1995	1.1994
fastslow	-40	-0.122	1.1993	1.1993
fastslow	0	-0.932	1.1994	1.1994
fastslow	25	1.2075	1.2002	1.2002
fastslow	85	63.789	1.1995	1.1993
slow	-40	47.3361	1.2034	1.2033
slow	0	2.019	1.2029	1.2029
slow	25	1.5026	1.2035	1.2035
slow	85	85.407	1.2022	1.2019
fast	-40	-1.0428	1.1944	1.1944
fast	0	-0.701	1.1953	1.1953
fast	25	1.3734	1.1963	1.1963
fast	85	22.3999	1.1965	1.1964
nom	-40	-1.5724	1.1993	1.1993
nom	0	-1.4105	1.1994	1.1994
nom	25	0.76	1.2002	1.2002
nom	85	41.1138	1.1995	1.1994

4.3. Monte Carlo analysis

The Monte Carlo test was performed using predefined analysis from the work environment. It predicts circuit performance due to process and mismatch variations.

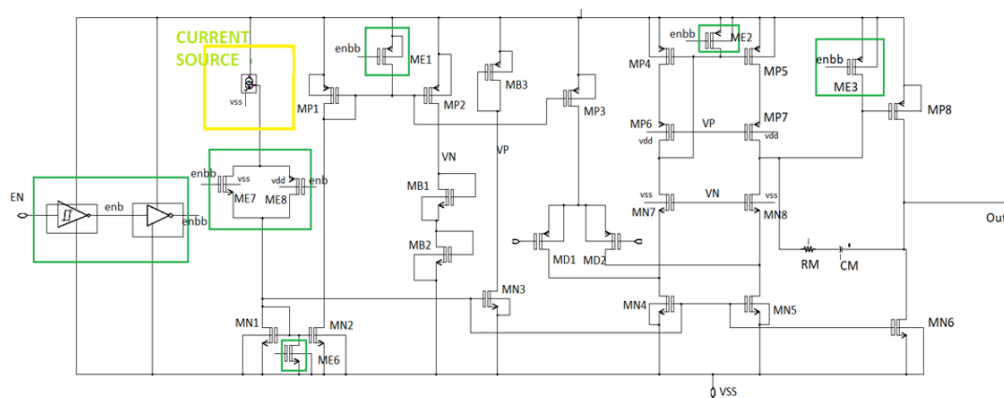


Fig. 20. The schematic of the operational amplifier.

There are multiple sources of error that can determine a large standard deviation for the reference voltage, the most noticeable being: resistive mismatch, mismatch of the current mirror and the offset of the operational amplifier.

Fig. 20 shows the schematic of the operational amplifier. No special techniques for compensating the offset voltage were implemented so far.

It was observed that most important source of error for the high value of standard deviation is the operational amplifier's offset voltage.

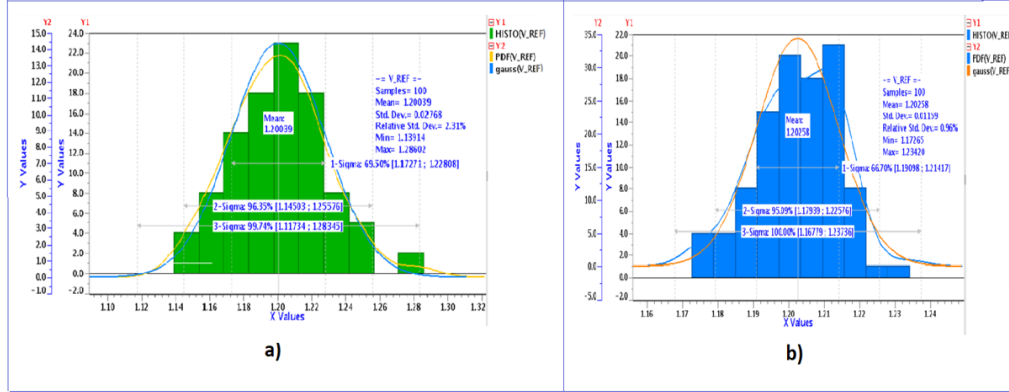


Fig. 21. MC analysis for the reference voltage. a) using a real amplifier b) using an ideal amplifier

The value of the standard deviation using an ideal operational amplifier was observed in Fig. 21b. Thus, it is observed that more than 50% of the reference voltage standard deviation is due to the operational amplifier's offset voltage.

The offset that appears in the operational amplifier affects the potentials at the points where its inputs are connected. Thus, the currents of CTAT and PTAT will vary from the designed ones. It will produce a different reference voltage and curvature over temperature. In case the offset reduction techniques will not prove to be sufficient, trimming techniques can be used to solve the issue. Trimming adjusts the resistors and hence the current back to design intent. In this way, the reference voltage will be the desired output voltage and the temperature performance will be the targeted one.

4.4. Comparison to state of the art

The results for proposed BVR and comparisons among several voltage references fabricated in standard CMOS process are listed in Table 5. Moreover, a figure of merit has been realised, given by (6).

$$FOM = \frac{TR}{TC \cdot VDD_{min} \cdot I_{cc}} \quad (6)$$

Where TR is the temperature range.

Table 5. BVR results and comparisons

Parameter	This work	[3]	[4]	[6]	[7]	[8]	Unit
V_{ref}	1.2	1.176	0.292	1.196	1.158	1.21	V
Max I_{cc}	22	50	40.6	38	186	68.25	μA
Best TC	5.9	13	9.9	4.81	2.36	1.65	ppm/ $^{\circ}C$
Temp range	-40 to 85	-40 to 140	-40 to 125	-5 to 125	-40 to 150	-40 to 125	C
Vdd range	1.65 to 3.6	1.7 to 1.9	1.6 to 4	2.1 to 5	2.6 to 6	4 to 7	V
Standard deviation	27.68	6.05	-	43.55	23	-	mV
Noise @ 1kHz	0.96	-	-	-	-	-	$\mu V/\sqrt{(Hz)}$
Technology	0.18	0.18	0.18	0.5	0.35	0.25	CMOS[μm]
Year reported	2021	2017	2019	2018	2014	2018	-
Figure of Merit	0.58	0.16	0.25	0.33	0.16	0.366	

Based on a figure of merit, it can be concluded that, compare to the other references, the circuit provides the best compromise regarding the temperature range, the minimum supply voltage, the total current consumption and the temperature coefficient.

5. Conclusions

To sum up, although bandgap voltage references are intensely used in multiple integrated circuits, the precise design of those blocks does require a lot of design time, as a result of numerous parameters that have to be properly chosen.

In the implementation of this bandgap voltage reference, the main purpose was to reduce the temperature coefficient, by segmenting the temperature range into multiple disjoint subintervals. The aim was to obtain three segments and for that it was necessary the introduction of two nonlinear currents, generated through the piece-wise linear technique.

Furthermore, multiple equations have been studied: the method for creating the 1st order reference, the generation technique for nonlinear currents as well as the way in which the parameters can be set or accordingly adjusted to obtain the targeted waveform at the output. Moreover, an algorithm was created which, by iteratively calculating slopes and through basic programming statements (“if” and “while”), calculated the desired coefficients and plotted all the waveforms from the beginning to the final one.

This code was created using MATLAB software and successfully calculated the desired design coefficients based on literature formula. Those values represented the beginning of the design process, and with small adjustments led to optimal results.

Multiple PVT simulations were done, which verified the temperature behaviour of the circuit, line sensitivity, the quiescent current as well as Monte Carlo analysis.

Thus, a low temperature coefficient BVR was designed and simulated in a 0.18 μm CMOS technology. The proposed circuit achieves a TC of less 6ppm/ $^{\circ}C$, with a maximum quiescent current of 22 μA , for supply voltages between 1.8V and 3.6V, over a temperature range of -40 $^{\circ}C$ to 85 $^{\circ}C$.

The bandgap voltage reference is intended for integration within a digital controlled output voltage stabilizer, being the reason of obtaining a small current consumption. The performance

can be improved by increasing this parameter.

The reference voltage is sensitive to process and mismatch variations. Post-fabrication trimming technique may be necessary in order to reduce the Monte Carlo standard deviation of the reference voltage. In this work, considering the block in which the circuit is integrated, the standard deviation of the reference circuit can be compensated by controlling the regulator's output.

Using this method, the design time was considerably reduced, and optimal results were achieved.

Acknowledgements. This work was supported by ON Semiconductor[®] Romania, giving access to resources and design platforms.

MATLAB is a registered trademark of The MathWorks, Inc. See mathworks.com/trademarks for a list of additional trademarks.

Pyxis[™] is a trademark of Mentor Graphics Corporation.

References

- [1] Madalina BONCU, Catalin BOTEZATU, Florin DRAGHICI, *A precise method for compensating bandgap references over temperature*, Proceedings of the Romanian International Conference on Semiconductors (CAS), 2020.
- [2] Gabriel Alfonso RINCON-MORA, *Voltage references; From Diodes to Precision High-Order Bandgap Circuits*, Texas Instruments Inc., 2002.
- [3] Michael HANHART, Ralf WUNDERLICH, Stefan HEINEN, *A 1.2 V Bandgap Reference with an additional 29.6 ppm/°C Temperature Stable Output Current*, PRIME 2017.
- [4] Radha MOTHUKURU, Manish KUMAR, and Bibhu Datta SAHOO, *A Curvature Compensated Bandgap Circuit Exploiting Temperature Dependence of β* , 7th International Conference on Modern Circuits and Systems Technologies, 2019.
- [5] Jonathan Felipe Perez CALVILLO, *Design of Bandgap Voltage Reference with Curvature Compensation for the Space Industry*, Thesis to obtain the Master of Science Degree in Electronics Engineering, October 2016.
- [6] Xin MING, Li HU, Yang-Li XIN, Xuan ZHANG, Di GAO, and Bo ZHANG, *A High-Precision Resistor-Less CMOS Compensated Bandgap Reference Based on Successive Voltage-Step Compensation*, IEEE **65**(12), Dec. 2018.
- [7] Iustin-Catalin NECULA, Cosmin RADU-POPA, *Voltage reference with Second Order Curvature Correction*, CAS 2014.
- [8] Hingjie LI, Lili, *A low-temperature drift and high-precision bandgap*, IMCEC 2018.
- [9] G.A. RINCON-MORA and P. E. ALLEN, *A 1.1-V Current-Mode and Piecewise-Linear Curvature-Corrected Bandgap Reference*, IEEE J. Solid-State Circuits **33**, pp. 1551–1554, Oct. 1998.